ARTICLE



Cortical hypometabolism in Parkinson's disease is linked to cholinergic basal forebrain atrophy

Miguel A. Labrador-Espinosa (1,2,3,4,12), Jesús Silva-Rodriguez (1,2,5,12), Niels Okkels^{6,7}, Laura Muñoz-Delgado (1,2), Jacob Horsager⁸, Sandra Castro-Labrador (1,2,5), Pablo Franco-Rosado (1,2), Ana María Castellano-Guerrero (1,2), Elena Iglesias-Camacho (1, Manuela San-Eufrasio (1), Daniel Macías-García (1,2), Silvia Jesús (1,2), Astrid Adarmes-Gómez (1,2), Elena Ojeda-Lepe (1,2), Fátima Carrillo (1,2), Juan Francisco Martín-Rodríguez (1,2), Florinda Roldan Lora (1,2), David García-Solís (1,2), Per Borghammer (1,2), Pablo Mir (1,2), Pabl

© The Author(s), under exclusive licence to Springer Nature Limited 2024

Cortical hypometabolism on FDG-PET is a well-established neuroimaging biomarker of cognitive impairment in Parkinson's disease (PD), but its pathophysiologic origins are incompletely understood. Cholinergic basal forebrain (cBF) degeneration is a prominent pathological feature of PD-related cognitive impairment and may contribute to cortical hypometabolism through cholinergic denervation of cortical projection areas. Here, we investigated in-vivo associations between subregional cBF volumes on 3T-MRI, cortical hypometabolism on [18F]FDG-PET, and cognitive deficits in a cohort of 95 PD participants with varying degrees of cognitive impairment. We further assessed the spatial correspondence of the cortical pattern of cBF-associated hypometabolism with the pattern of cholinergic denervation in PD as assessed by [18F]FEOBV-PET imaging of presynaptic cholinergic terminal density in a second cohort. Lower volume of the cortically-projecting posterior cBF, but not of the anterior cBF, was significantly associated with extensive neocortical hypometabolism [p(FDR) < 0.05], which mediated the association between cBF atrophy and cognitive impairment (mediated proportion: 43%, p < 0.001). In combined models, posterior cBF atrophy explained more variance in cortical hypometabolism ($R^2 = 0.26$, p < 0.001) than local atrophy in the cortical areas themselves ($R^2 = 0.16$, p = 0.01). Topographic correspondence analysis with the [18F]FEOBV-PET pattern revealed that cortical areas showing most pronounced cBF-associated hypometabolism correspond to those showing most severe cholinergic denervation in PD (Spearman's $\rho = 0.57$, p < 0.001). In conclusion, posterior cBF atrophy in PD is selectively associated with hypometabolism in denervated cortical target areas, which mediates the effect of cBF atrophy on cognitive impairment. These data provide first-time in-vivo evidence that cholinergic degeneration represents a principle pathological correlate of cortical hypometabolism underlying cognitive impairment in PD.

Molecular Psychiatry; https://doi.org/10.1038/s41380-024-02842-9

INTRODUCTION

Cognitive impairment represents one of the most common and incapacitating non-motor symptoms among the diverse range of clinical manifestations in Parkinson's disease (PD) [1]. Cortical dysfunction as measured by hypometabolism on [¹⁸F]fluorodeoxyglucose (FDG) PET is a well-established neuroimaging correlate of cognitive impairment in PD [2, 3]. Interestingly, cortical hypometabolism in PD and related Lewy body disorders typically drastically exceeds the degree of cortical neurodegeneration as measured by structural MRI [3, 4], and it has been hypothesized that cortical dysfunction in these disorders may be primarily driven by the loss of subcortical input projections rather than by local neurodegenerative processes [5, 6]. Specifically,

degeneration of cholinergic basal forebrain (cBF) neurons is known to be a major contributor to the cognitive impairments associated with PD [7], and it may contribute to cortical dysfunction through cholinergic denervation of the cBF's widespread cortical projection areas [8, 9]. Supporting the hypothesis of a cholinergic influence on cortical hypometabolism in PD-related cognitive decline, animal experiments have shown that selective cBF lesions can induce hypometabolism in the cholinergically denervated cortical regions, which mediates the effect of cBF lesions on ensuing cognitive impairment [10, 11].

Using novel imaging biomarkers such as cBF volume derived from magnetic resonance imaging (MRI), previous studies by us and others have established robust in vivo associations between

¹Unidad de Trastornos del Movimiento, Servicio de Neurología y Neurofisiología Clínica, Instituto de Biomedicina de Sevilla, Hospital Universitario Virgen del Rocío/Universidad de Sevilla/CSIC/CIBERNED, Sevilla, Spain. ²Centro de Investigación Biomédica en Red sobre Enfermedades Neurodegenerativas (CIBERNED), Instituto de Salud Carlos III, Madrid, Spain. ³Department of Psychiatry and Neurochemistry, Institute of Physiology and Neuroscience, University of Gothenburg, Gothenburg, Sweden. ⁴Wallenberg Centre for Molecular and Translational Medicine, University of Gothenburg, Gothenburg, Sweden. ⁵Reina Sofia Alzheimer Centre, CIEN Foundation, ISCIII, Madrid, Spain. ⁶Department of Neurology, Aarhus University Hospital, Aarhus, Denmark. ⁷Department of Neurology, Regional Hospital Viborg, Viborg, Denmark. ⁸Department of Nuclear Medicine and PET, Aarhus University Hospital, Aarhus, Denmark. ⁹Unidad de Radiodiagnóstico, Hospital Universitario Virgen del Rocío, Sevilla, Spain. ¹⁰Unidad de Medicina Nuclear, Hospital Universitario Virgen del Rocío, Sevilla, Spain. ¹²These authors contributed equally: Miguel A. Labrador-Espinosa, Jesús Silva-Rodriguez. [™]email: pmir@us.es; mgrothe@fundacioncien.es

Received: 11 April 2024 Revised: 4 November 2024 Accepted: 11 November 2024

Published online: 05 December 2024

decreased cBF volume and cognitive impairments in patients with early and advanced PD [12, 13]. In addition, atrophy of the cBF has also been found to predict longitudinal cognitive decline in early-stage PD [14–17]. However, to date, a potential link between cBF degeneration and cortical hypometabolism in the context of PD-related cognitive impairment is yet to be investigated.

In the present study, we used combined MRI and [¹⁸F]FDG PET imaging to investigate in vivo associations between cBF degeneration and regional cortical hypometabolism in a large sample of PD participants with varying degrees of cognitive impairment, and we further assessed whether cBF-associated cortical hypometabolism mediates the association of cBF atrophy with cognitive deficits. Additionally, we studied whether the regional pattern of cBF-associated cortical hypometabolism corresponds to cortical areas of most pronounced cholinergic denervation in PD as revealed by PET imaging of presynaptic cholinergic terminal density using [¹⁸F]fluoroethoxybenzovesamicol (FEOBV), a novel radiotracer specific to the vesicular acetylcholine transporter (VAChT).

MATERIALS AND METHODS

Participants

Our main cohort included ninety-five PD participants with varying degrees of cognitive impairment, recruited by the Movement Disorders Clinic at the University Hospital 'Virgen del Rocío' in Seville, Spain. PD was diagnosed according to the clinical diagnostic criteria of the Movement Disorder Society (MDS) [18]. Participants underwent comprehensive cognitive assessments in the presence of dopamine replacement medication ('on' state) as well as multimodal neuroimaging scans (MRI and [18F]FDG PET). Participants potentially subjected to factors (other than PD) that could contribute to cognitive impairment (including other primary neurological diseases, major psychiatry disorders, or major depression) or with contraindications to MRI or PET were excluded.

Our study also included a second cohort consisting of 15 PD participants and 15 cognitively intact healthy elderly controls who underwent [¹⁸F] FEOBV PET imaging at the Department of Nuclear Medicine and PET at Aarhus University Hospital, Denmark. The detailed selection criteria for this second cohort have been described in detail in a previous report [19] and clinical descriptions are summarized in supplementary Table S1.

The study was approved by the Ethics Committee of the University Hospital 'Virgen del Rocío' (approval number: 2158-N-20) according to the guidelines of the Helsinki declaration, and written informed consent was obtained from all study participants. Recruitment of both cohorts was conducted between January 2019 and December 2022.

Clinical and neuropsychological assessment

Disease stage and motor symptom severity in 'off' state were assessed using the Hoehn and Yahr (H&Y) scale and the Unified Parkinson's Disease Rating Scale - Part III (UPDRS III).

Cognitive performance was assessed using the Montreal Cognitive Assessment (MoCA) and the Parkinson's Disease-Cognitive Rating Scale (PD-CRS) [20]. The total PD-CRS score (PD-CRS_{Total}) was used as our primary outcome measure for cognitive impairment, but we also included additional analyses of the 'fronto-subcortical' and 'posterior-cortical' PD-CRS summary scores [21]. The fronto-subcortical subscore includes the sum of item scores from tests of sustained attention, working memory, alternating and action verbal fluency, immediate and delayed verbal memory, and clock drawing. The posterior-cortical subscore includes the sum of item scores from tests of naming and clock copying. Based on the PD-CRS_{Total} score, PD participants were classified into cognitive groups using previously established cut-offs [20]. Participants with PD-CRS_{Total} > 81 were categorized as having normal cognition (PD-CN), participants with PD-CRS_{Total} ≤ 81 but >64 were classified as having mild cognitive impairment (PD-MCI), and individuals with PD-CRS_{Total} ≤ 64 as well as evidence of functional impairment in activities of daily living were classified as having dementia (PDD).

Alzheimer's disease biomarkers

For a better characterization of our study sample in terms of Alzheimer's disease (AD) co-pathology, we determined plasma levels of tau phosphory-lated at threonine 217 (P-tau217) [22] as well as the prevalence of the APOE-

ε4 genotype. These data were only measured in a subset of the analyzed cohort (94% P-tau217; 82% APOE-ε4). Briefly, plasma P-tau217 levels were measured using the novel ALZpath single molecule array (SIMOA) assay, and biomarker status (abnormal vs normal) was determined using a predefined cutoff of 0.40 pg/mL as previously described [23]. APOE-ε4 positivity was determined using Taqman SNP Genotyping Assays (Applied Biosystems, Foster City, CA) in a LightCycler480-II (Roche Applied Science, Penzberg, Germany) [24].

Multimodal neuroimaging acquisitions

For the main cohort, MRI acquisitions were performed on a 3T Philips Ingenia scanner. A 3D T1-weighted turbo field echo (TFE SENSE) sequence produced high-resolution structural images with the following parameters: repetition time = 8.2 ms, echo time = 3.75 ms, flip angle = 8°, fleid of view = 240×240 mm, acquisition matrix = $256 \times 256 \times 180$ slices, voxel size = $0.94 \times 0.94 \times 1.00$ mm³. The image plane was positioned sagittally along the hemispheric fissure and axially along the anterior/posterior commissure plane. Regarding [18 F]FDG PET, participants were scanned for 20 min starting 45 min after the injection of ~200 Mbq of [18 F]FDG. [18 F] FDG PET acquisitions were performed on two different scanners, a Siemens BioGraph HiRes (17 participants) and a GE Discovery MI (78 participants). In order to increase signal homogeneity across the different scanners a differential smoothing approach was applied (Siemens: 4.5 mm, GE: 6.5 mm). Differential smoothing values were calculated using a previously validated resolution estimation method [25, 26].

For the second cohort, $[^{18}F]FEOBV$ PET images were acquired for 30 min starting 180 min after injection of ~200 MBq of $[^{18}F]FEOBV$. Images were acquired on a Siemens BioGraph Vision 600 PET/CT scanner. Image reconstruction of all PET images was performed using the 3D iterative reconstruction methods available for each scanner, including corrections for attenuation, scatter, and random coincidences.

Neuroimaging data processing

A flowchart summarizing the neuroimaging processing pipeline used in our study is provided in supplementary Fig. S1. Automated cBF volumetry on T1-weighted structural MRI scans followed established processing procedures using Statistical Parametric Mapping software (SPM12, Wellcome Trust Center for Neuroimaging) and the Computational Anatomy Toolbox (CAT12 v12.8, Jena University Hospital) as previously described [12, 14]. Briefly, T1-weighted MRI scans were segmented into grey matter (GM), white matter, and cerebrospinal fluid partitions and GM segmentations were high-dimensional spatially normalized to Montreal Neurological Institute (MNI) standard space, including modulation of voxel values to account for the volumetric changes induced by the spatial transformation [27]. GM volumes of the cBF were then automatically extracted by summing up the modulated GM voxel values within distinct anterior and posterior cBF regions of interest (ROIs), as defined by a previous methodological study characterizing functionally homogeneous subdivisions within the human cBF [12, 28]. The posterior cBF subdivision primarily corresponds to the cytoarchitectonic subregion of the nucleus basalis of Meynert, which provides the principle of source of cholinergic projections to the neocortex, while the anterior cBF subdivision corresponds to the medial septum and diagonal band of Broca, which send more selective cholinergic projections to the hippocampus and related limbic structures [8, 9]. Total intracranial volume (TIV) was calculated as the sum of the total volumes of the GM, white matter, and

cerebrospinal fluid partitions.

Processing of [¹⁸F]FDG PET scans followed our established in-house pipeline that have been described in detail previously [29, 30]. Each subject's [¹⁸F]FDG PET scan was rigidly co-registered to the corresponding structural MRI scan and corrected for partial volume effects (PVEs) using the Müller–Gärtner method implemented in the PETPVE12 toolbox in SPM12 [31]. PVE-corrected [¹⁸F]FDG PET scans were warped to the MNI reference space using the deformation fields derived from the normalization of the corresponding MRI scans. Normalized [¹⁸F]FDG PET scans were intensity-scaled using a pons reference region to generate standardized uptake value ratio (SUVR) maps. Finally, for voxel-wise analyses normalized [¹⁸F]FDG PET SUVR images were smoothed using an 8-mm isotropic smoothing kernel.

For the second cohort, [18F]FEOBV PET images were processed using a slightly different but analogous processing pipeline as previously established for this novel tracer [19, 32]. Briefly, each subject's [18F]FEOBV PET scan was co-registered with a corresponding structural MRI scan and

Table 1. Demographic, clinical, and cognitive characteristics.

Variables	Descriptive statistics
N	95
Gender, Female/Male (F%)	24/71 (25%)
Age, years	65.1 (9.4)
Higher education, Yes/No (Yes %)	35/60 (37%)
Age at onset, years	57.8 (8.7)
Disease duration, years	7.2 (4.3)
H&Y, stages	2 (1 - 4)
UPDRS-III-Off, scores	24.9 (12.6)
MoCA, scores	21.1 (6)
PD-CRS, total scores	76.9 (24.9)
Fronto-subcortical subscore	50.3 (21.9)
Posterior-cortical subscore	26.6 (4)
Cognitive category, PD-CN/PD-MCI/PDD	41/27/27

The descriptive values presented are: counts (percentage) for categorical variables; median (IQR) for Hoehn & Yahr stage; and mean (standard deviation) for all other continuous variables. Higher education refers to more than 12 years of formal education.

N number of PD participants, H&Y Hoehn & Yahr, UPDRS-III-off Unified Parkinson's disease rating scale - Part III in "Off" state, PD-CRS Parkinson's disease - cognitive rating scale, MoCA Montreal cognitive assessment, PD-NC PD participants with normal cognition, PD-MCI PD participants with mild cognitive impairment, PDD PD participants with dementia.

corrected for PVEs using the Müller–Gärtner method. Images were transformed into the MNI standard space, intensity-scaled using the centrum semiovale as the reference region and smoothed with a Gaussian kernel of 10-mm.

Statistical analysis

Associations between cBF atrophy and cortical hypometabolism were assessed using voxel-wise regression analyses of anterior and posterior cBF volumes on [18F]FDG PET SUVR maps, controlling for volume of the other cBF subregion (posterior or anterior, respectively), sex, education, TIV, scanner model, and cognitive category. Analysis was restricted to a binary mask of the cortical GM and results are presented as partial r maps, thresholded at P < 0.05 (FDR-corrected). To better understand the differential contributions of cBF atrophy versus local cortical degeneration to cortical hypometabolism in PD, we calculated an additional multivariate regression model that incorporates both cBF volume and local cortical GM volume as joint predictor variables for cortical hypometabolism. To this end, we calculated individual GM volumes of the cortical regions that showed a significant association between cBF volume and hypometabolism. This measure was obtained by summing up the voxel-wise (modulated) GM volumes within the mask of cortical regions where regional metabolism was significantly correlated with posterior cBF volume. Similarly, the mean cortical SUVR value of these cBF-related regions was calculated for each individual. Differences in the explained variance of cBF volume and local cortical GM volume on cortical hypometabolism were then examined by decomposed R² indices for each variable in the full model [33].

After establishing a specific link between cBF atrophy and cortical hypometabolism, we used path analyses to further investigate whether the association between cBF atrophy and cognitive impairment in PD is mediated by cortical hypometabolism [29]. Mediation models were calculated using cBF volume as the causal variable, cognitive performance (PD-CRS_{Total}) as the outcome variable, and cBF-related cortical hypometabolism as the mediator variable. In these models, cBF-related cortical hypometabolism was calculated as the weighted average cortical SUVR across voxels showing a significant association with cBF volume, using the effect size of the association with cBF volume as the weights for each voxel. Path analyses of the average direct effect (ADE, direct effect of CBF atrophy on cognitive deficits), the average causal mediation effect (ACME, indirect effect of cBF atrophy on cognitive deficits that is mediated by cortical hypometabolism), and the mediated proportion were assessed

using non-parametric bootstrap with 1000 resamples [34]. All association analyses were performed using linear regression models adjusted for age, sex, education, cognitive category (for the association between cBF atrophy and cortical hypometabolism), TIV (when using MRI-based volume variables), and PET scanner (when using PET-based variables). The PD-CRS_{Total} score was used as the primary cognitive variable for all analyses, but additional mediation models were calculated for the fronto-subcortical and posterior-cortical subscores of the PD-CRS. Sensitivity analyses were performed to evaluate the potential relation of the observed effects with disease severity, using regression models additionally accounting for years of disease duration and motor symptom severity as measured by UPDRS-Ill-off score, as well as using regression models that excluded PD participants with dementia.

Finally, we assessed differences in regional [¹⁸F]FEOBV PET SUVR values between PD participants and healthy controls from the second cohort using 2-sample *t*-tests across 100 distinct ROIs covering the whole cortical GM as defined in the functional parcellation atlas by Schaefer et al. [35]. In order to formally quantify the topographic correspondence between the cortical patterns of cBF-associated cortical hypometabolism and cholinergic denervation in PD, we then performed spatial (Spearman's) correlation analysis between the regional degree of cBF-associated hypometabolism (partial *r*) and the regional degree of cholinergic denervation (*t*-values from [¹⁸F]FEOBV PET analysis) across these 100 cortical ROIs.

All statistical analyses were performed using R software (R Foundation for Statistical Computing, V4.1.0). Mediation models were conducted using the mediation package v4.5.0. Voxel-wise analyses were performed using SPM12 in Matlab R2018a.

RESULTS

Clinical characteristics

Demographic, clinical, and cognitive characteristics of the PD participants are detailed in Table 1. PD participants had an average age of 65 ± 9 years, were predominantly male (75%), and had a mean disease duration of 7.2 ± 4.3 years. Cut-off criteria for the PD-CRS $_{Total}$ score revealed a notable cognitive diversity within the sample: 54 PD participants (57%) exhibited clinically relevant cognitive impairment, with 27 PD participants being categorized as PD-MCI and an equal number of 27 PD participants meeting criteria for PDD.

Within the subsample of PD participants with available AD biomarker data, 21% (19/89) had abnormal plasma P-tau217 levels and 15% (12/78) were APOE-£4 positive.

Posterior cBF atrophy associates with cortical hypometabolism in PD

In voxel-wise regression analyses adjusted for multiple comparisons, posterior cBF volume was significantly associated with extensive cortical hypometabolism, covering lateral and medial fronto-parietal regions, the lateral temporal lobe, inferior and medial parietal areas, and occipital regions (Fig. 1). By contrast, the anterior cBF volume was only associated with hypometabolism in the anterior cBF itself and closely adjacent regions, and these effects did not survive correction for multiple comparisons (supplementary Fig. S2).

In additional analyses assessing the influence of local cortical atrophy, local cortical GM volume was calculated by the sum of voxel-wise GM volumes in the cortical regions where regional metabolism was significantly associated with posterior cBF volume (see supplementary Fig. S3 and supplementary Table S2). Combining both posterior cBF volume and local cortical GM volume into a multimodal regression model for cortical hypometabolism slightly increased the fit compared to the model based on cBF volume alone (Global R^2 : 0.468 vs. 0.503, $\Delta R^2 = 0.035$ (7.5%), p = 0.01). However, although local cortical GM volume was also a significant predictor of cortical hypometabolism in this model (t = 2.51, p = 0.01, decomposed $R^2 = 0.16$, 31% of total explained variance), posterior cBF volume showed a considerably stronger influence (t = 4.42, p < 0.001, decomposed $R^2 = 0.26$, 52% of total explained variance).

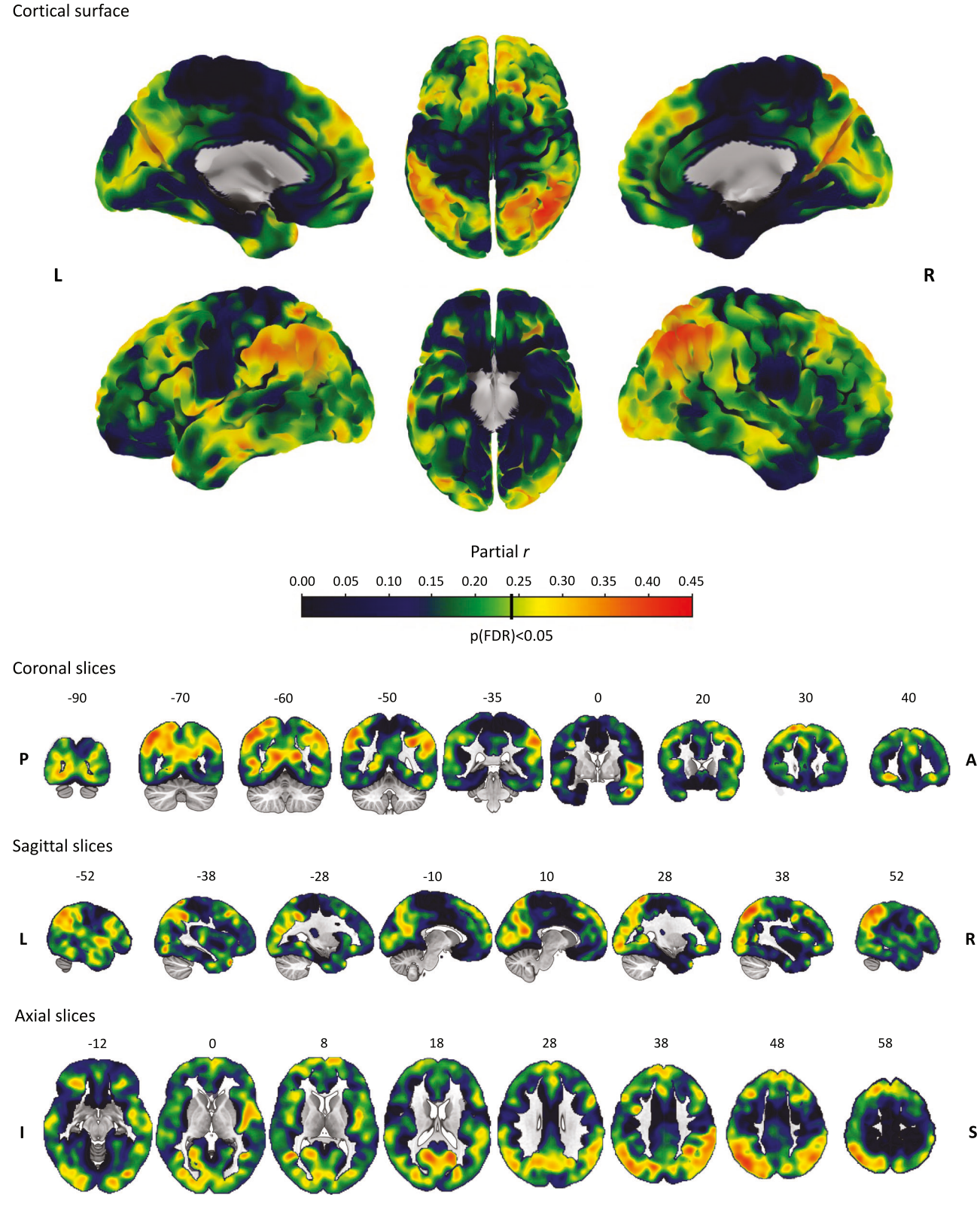


Fig. 1 Associations between posterior cBF atrophy and cortical hypometabolism in PD. The figure shows regional effects of voxel-wise regression analyses of posterior cBF volume on cortical hypometabolism in PD participants, controlled for anterior cBF volume, sex, age, education, TIV, PET scanner, and cognitive category. Effects are depicted on cortical surfaces showing medial, lateral, superior, and inferior brain renderings; coronal slices from posterior to anterior; sagittal slices from left to right; and axial slices from inferior to superior. The black vertical bar in the color scale of partial r values denotes the effect size corresponding to a statistical threshold of p(FDR) < 0.05.

SPRINGER NATURE Molecular Psychiatry

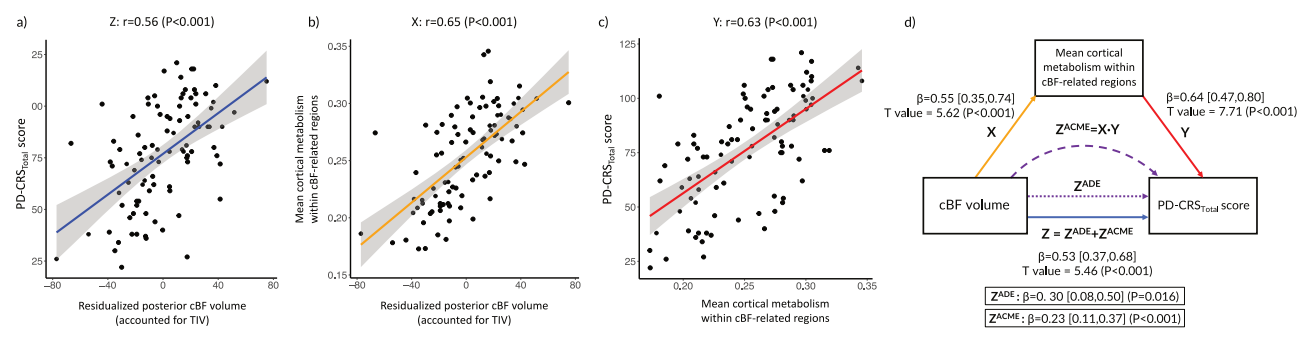


Fig. 2 Mediation analysis of associations between cBF atrophy, cortical hypometabolism, and cognitive impairment. a Residualized posterior cBF volume (x-axis) plotted against PD-CRS_{Total} score (y-axis). Blue line represents linear trend; (\mathbf{b}) Residualized posterior cBF volumes (x-axis) plotted against average cortical hypometabolism in cBF-related cortical areas (y-axis). Orange line represents linear trend; (\mathbf{c}) Average cortical hypometabolism in cBF-related cortical areas (y-axis) plotted against PD-CRS_{Total} score (x-axis). Red line represents linear trend; Pearson's r values obtained from the direct correlation between variables are displayed. d Path diagram of the causal mediation model where the effect of cBF atrophy on cognitive impairment is plotted in path Z (blue arrow), the effect of cBF atrophy on cortical hypometabolism is plotted in path X (orange arrow), and the effect of cortical hypometabolism on cognitive impairment is plotted in path Y (red arrow). Standardized betas [95% confidence intervals], T values and P values of the regression analyses are indicated separately for each association. The total effect of path Z is composed by the sum of the average direct effect (Z^{ADE}) and the average causal mediation effect (Z^{ACME}) (purple arrows).

cBF-associated cortical hypometabolism mediates the association between cBF atrophy and cognitive impairment in

In covariate-controlled regression models, lower posterior cBF volume was significantly associated with worse PD-CRS_{Total} scores $(r_{\text{partial}} = 0.36, p = 0.001)$. By design, lower posterior cBF volume was also significantly associated with average cortical hypometabolism in cBF-associated areas ($r_{partial} = 0.40$, p < 0.001) (Fig. 2a, b). In addition, cBF-associated cortical hypometabolism was also significantly associated with worse PD-CRS_{Total} scores ($r_{partial}$ = 0.40, p < 0.001). Interestingly, path analyses showed that 43% of the total effect of posterior cBF atrophy on cognitive impairment (total effect: $\beta = 0.53$ [0.37,0.68], p < 0.001) was mediated by cBFassociated cortical hypometabolism (ADE: $\beta = 0.30$ [0.08,0.50], p = 0.016; ACME: $\beta = 0$. 23 [0.11,0.37], p < 0.001; mediated proportion: 43%, p < 0.001) (Fig. 2c, d). Significant mediator effects of cBF-associated cortical hypometabolism were also observed for associations between posterior cBF atrophy and cognitive deficits in the fronto-subcortical and the posterior-cortical subscores of the PD-CRS (supplementary data S1).

In further sensitivity analyses evaluating the potential relation of the observed effects with disease severity, similar associations were observed using regression models that additionally controlled for years of disease progression and motor symptom severity. Moreover, all the observed associations remained significant when using regression models restricted to PD participants without dementia (supplementary data S2).

cBF-associated cortical hypometabolism corresponds to areas

of pronounced cholinergic denervation in PDRegional differences in [¹⁸F]FEOBV uptake between PD participants and healthy controls in cohort 2 are illustrated in Fig. 3a. Differences were particularly notable in lateral and medial posterior parieto-temporo-occipital areas and in the lateral superior frontal lobe. Visual comparison revealed a regional pattern remarkably similar to the pattern of cBF-associated cortical hypometabolism in our main cohort (Fig. 3b). Formal topographic correspondence analysis revealed a strong spatial correlation between both patterns (Spearman's $\rho = 0.57$, p < 0.001) (Fig. 3c).

DISCUSSION

In the present multimodal MRI-PET imaging study, we investigated in vivo associations between cBF atrophy, cortical hypometabolism, and cognitive impairment in a large sample of PD participants. We also examined the spatial correspondence of the observed pattern of cBF-associated cortical hypometabolism with areas of most pronounced cortical cholinergic denervation in PD as measured by [18F]FEOBV PET. We found that posterior cBF atrophy was closely associated with extensive cortical hypometabolism in fronto-parietal, lateral temporal, and occipital regions, which partially mediated the association between cBF and cognitive impairment. Interestingly, these anatomically remote associations were specific for the cortically-projecting posterior cBF as no comparable associations were observed for the anterior cBF. Moreover, cortical areas showing hypometabolism associated with posterior cBF atrophy overlapped with those areas estimated to undergo most pronounced cholinergic denervation in PD.

Recent in vivo MRI studies have revealed robust associations between cBF degeneration and cognitive decline in PD patients [12-16]. In another line of research, cortical hypometabolism as measured by [18F]FDG PET has long been known to closely track with cognitive impairment in PD [2, 3, 36]. Taken together with the strong influence of cholinergic innervation on cortical synaptic function and cognition [8, 37], these findings suggest that cBF atrophy and cortical hypometabolism may be interrelated phenomena in PD that are pathophysiologically linked to cognitive impairment. Research in experimental animal models has demonstrated that selective cholinergic lesions in the basal forebrain can induce hypometabolism in denervated cortical areas that correlates with cognitive deficits [10, 11]. In humans, neuropathologic studies of patients with Parkinson's or Alzheimer's disease have described strong relationships between the loss of cholinergic cBF neurons and degenerative changes in cortical target areas [38, 39]. Moreover, more recent neuroimaging studies of patients with AD could demonstrate in vivo associations between cBF degeneration and hypometabolism in highly innervated cortical target areas of the cBF projections [29]. Here, we demonstrate that a similar in vivo association between cBF atrophy and cortical hypometabolism is also present in PD patients and that these processes are interrelated in their contribution to cognitive impairment.

Although not directly assessed in our study, an underlying assumption of our analyses is that the associations between cBF atrophy and cortical hypometabolism may represent a functional consequence of cortical cholinergic denervation. In support of this hypothesis, we observed that cortical hypometabolism was specifically associated with atrophy in the posterior cBF ROI, which largely corresponds to the nucleus basalis of Meynert representing the main source of cholinergic projections to the

Molecular Psychiatry **SPRINGER NATURE**

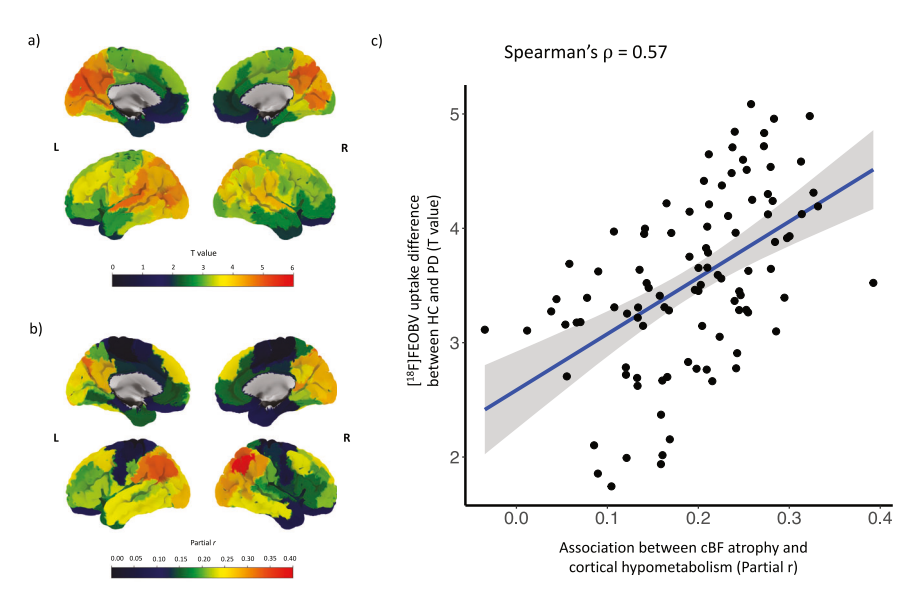


Fig. 3 Topographic correspondence between patterns of cBF-associated cortical hypometabolism and cholinergic denervation in PD. The figure shows the formal topographic correspondence between patterns of posterior cBF-associated cortical hypometabolism and cholinergic denervation in PD participants. **a** *T* values reflecting the difference in [¹⁸F]FEOBV uptake between groups of healthy controls and PD participants and (**b**) mean partial *r* values of the association between cBF atrophy and cortical hypometabolism are depicted on cortical surfaces displaying medial and lateral brain renderings. Regional mean values were calculated across 100 ROIs covering the entire cortical grown matter [35]. **c** An accompanying scatter plot illustrates the correlation between both measures across all cortical ROIs, demonstrating more pronounced cBF-associated hypometabolism (partial *r* values, *x*-axis) in regions with more severe cholinergic denervation (*T* value of [¹⁸F] FEOBV uptake differences, *y*-axis). Note that the [¹⁸F]FDG and [¹⁸F]FEOVB PET patterns used here were derived from two separate cohorts of PD participants.

neocortex [28, 37]. By contrast, atrophy of the anterior cBF ROI, corresponding to the medial septum and diagonal band of Broca, did not show significant associations with widespread neocortical hypometabolism, but rather selective association with hypometabolism in the anterior cBF itself and closely adjacent regions.

Interestingly, recent studies combining the same MRI-based cBF volume measurements used here with PET-based imaging of cholinergic neurotransmission in PD demonstrated that degeneration of the cBF, and particularly its posterior subregion, is indeed closely linked to a depletion of cholinergic activity in parieto-temporo-occipital areas [40-42]. Here, we add to this literature by demonstrating in a spatial correlation analysis that cBF-associated cortical hypometabolism is predominantly observed in those cortical areas that undergo most pronounced cholinergic denervation in PD, as assessed by using novel [18F] FEOBV PET imaging [5]. However, it is important to note that the [18F]FDG and [18F]FEOVB PET patterns used here were derived from two different cohorts, and combined multi-tracer [18F]FDG and [18F]FEOVB PET studies are needed to substantiate these data using individual-level analyses of the relation between cortical cholinergic denervation and hypometabolism.

While our analysis shows that cBF atrophy is strongly associated with cortical hypometabolism, this does of course not imply that cortical hypometabolism in PD is exclusively related to cholinergic degeneration. Particularly, cortical hypometabolism may also reflect local neurodegenerative processes in the cortex itself, and previous studies have suggested that cortical hypometabolism in PD is closely followed by macrostructural cortical atrophy as measured by reduced GM volumes on MRI [3]. However, in our additional analyses assessing the relative contributions of cBF degeneration and local cortical atrophy on cortical hypometabolism, we observed that remote cBF atrophy had a much stronger influence on cortical hypometabolism compared to co-localized cortical GM atrophy. This finding aligns with a growing body of evidence suggesting that cortical dysfunction in Lewy body disorders may be influenced more by the loss of cholinergic innervation and other neurochemical disturbances than by local neurodegenerative processes in the cortex itself [5, 6, 43–45]. In this line, a recent multi-tracer PET study found that cortical hypometabolism in Lewy body disorders by far exceeds the degree of cortical synaptic loss as estimated by PET imaging with the synaptic vesicle glycoprotein 2A (SV2A) radiotracer [11C]UCB-J, reinforcing that cortical hypometabolism is at least partly driven by remote processes rather than by local synaptic degeneration [46]. This also likely explains the typical dissociation between marked cortical hypometabolism and comparably preserved cortical GM structure in PD patients with cognitive impairment that is observed across neuroimaging studies [47] and may have critical implications for the development of clinically useful neuroimaging biomarkers for predicting cognitive decline in PD [48]

In our study, both cBF atrophy and cortical hypometabolism were found to be associated with cognitive impairment in PD participants, and further path analyses could demonstrate that the link between cBF atrophy and cognitive impairment was mediated by cortical hypometabolism. These findings support previous evidence linking both cortical hypometabolism and cholinergic degeneration with cognitive impairment in PD [2, 12, 40]. In additional analyses, we found similar associations of cBF atrophy and mediating effects of cortical hypometabolism with both the fronto-subcortical and posterior-cortical PD-CRS summary measures. This contrasts with predictions of the dual syndrome hypothesis, which suggests that cholinergic deficits in PD may be more closely associated with deficits in posterior-cortical cognitive domains than with fronto-subcortical cognitive domains, which are supposed to be more dependent on dopamine levels [1, 49]. However, consistent with our current findings, previous PET-based studies of cholinergic degeneration in non-demented PD patients have also shown a link between cortical cholinergic loss and impaired cognitive function across multiple cognitive domains, including classic fronto-subcortical domains such as attention and executive function [40, 50, 51]. A possible explanation for these discrepancies could be that the relative impact of cholinergic degeneration on cognitive functions may change during disease

SPRINGER NATURE Molecular Psychiatry

progression. Thus, more subtle cholinergic dysfunction may affect executive and attentional functions in early disease stages, whereas effects on more posterior cortical functions such as visuospatial abilities may only become apparent with more pronounced cholinergic degeneration as the disease progresses towards dementia.

Interestingly, we observed similar associations between cBF atrophy, cortical hypometabolism, and cognitive impairment when limiting our sample to PD participants without dementia, indicating that these processes are already relevant for early cognitive disturbances in PD. Together with other recent clinical research on cholinergic system degeneration in non-demented PD patients [12, 14, 17, 40, 41], these findings may warrant a reevaluation of the role of cholinergic treatment in predementia stages of PD [7]. Treatment with acetylcholinesterase inhibitors is well known to improve cognitive symptoms in patients with PDD and related Lewy body dementias, and this improvement has also been found to be linked to restoration of cortical metabolism [52-54]. However, clinical trials assessing the efficacy of cholinergic treatments for cognitive impairments in the pre-dementia stage of PD have presented inconsistent results [55], which could be related to the high variability in the degree of cholinergic degeneration in this population [56]. Consequently, neuroimaging markers of cholinergic system degeneration and associated cortical hypometabolism may help to select participants for clinical trials in PD, focusing on those patients at greatest risk for cognitive decline and most likely to benefit from cholinergic therapy.

The pattern of cBF-associated cortical hypometabolism in our PD sample shows some overlap with cortical areas that are typically affected in AD, particularly considering parietal areas, although the overall correspondence is rather limited, as an AD characteristic pattern typically shows a stronger involvement of medial parietal and medial temporal areas and less involvement of occipital and frontal areas compared to the pattern of cBFassociated hypometabolism detected in our study [57-59]. In our previous study using CSF biomarker data from the PPMI cohort, we found that both longitudinal cBF degeneration and its association with cortical atrophy in PD were largely independent of amyloid-\beta status, indicating that these processes are proper features of PD pathophysiology [17]. In our current study, positivity for both plasma P-tau217 levels and APOE-ε4 genotype were within the reported range for healthy elderly controls [60-62], indicating that our analyzed PD cohort is not particularly enriched for AD co-pathology. Together, this argues against the possibility that comorbid AD pathology may have a major influence on the findings in our current study. Accordingly, in a complementary analysis excluding the P-tau217 positive participants, lower posterior cBF volume remained significantly associated with cortical hypometabolism in this subsample $(r_{\text{partial}} = 0.36, p = 0.004)$. While out of the scope of the present study, future research studying in more detail the effect of AD biomarkers and risk genotypes on neuroimaging findings in PD may provide critical insights into the diverse pathological influences on regional neurodegeneration patterns and cognitive phenotypes in PD and other Lewy body diseases [63].

Our study also presents some limitations that should be considered. First, the lack of multimodal MRI-PET neuroimaging data of a healthy control group restricts the specificity of the observed effects to patients in the PD continuum. However, previous research had already demonstrated that variation in cBF volume due to the normal aging process is not associated with comparable effects on cortical hypometabolism or cognitive function [29]. Second, assumptions about the chain of events between cBF atrophy, cortical hypometabolism, and cognitive impairment are based on cross-sectional correlations from which

causality cannot be inferred. Third, cortical cholinergic signaling has not been directly assessed in this study and its role in the observed associations remains to be investigated in more detail. cBF volume on MRI is only an indirect structural marker of cholinergic system degeneration, although accumulating evidence from multimodal biomarker studies indicates that it is indeed closely related to cholinergic system function as assessed by neurophysiologic [64] or molecular imaging markers of cholinergic system integrity [40-42]. Finally, cholinergic system degeneration in PD does not occur in isolation but together with degenerative changes in the dopaminergic and other ascending neurotransmitter systems, which may also affect cortical hypometabolism but were not specifically assessed in our study [6, 65-67]. Multi-tracer PET studies are needed to better understand the unique and interactive contributions of neurotransmitter disturbances to cortical dysfunction and cognitive impairment in PD.

In conclusion, in this multimodal imaging study, we provide evidence for a close link between in vivo cBF degeneration and cortical hypometabolism in PD-related cognitive decline. The detected associations may have important implications for the design of clinically useful imaging biomarkers for disease prognosis and clinical trial stratification.

DATA AVAILABILITY

The data generated and analysed in the current study are available from the corresponding authors upon reasonable and formal request approved by the relevant local ethics committees.

REFERENCES

- Aarsland D, Batzu L, Halliday GM, Geurtsen GJ, Ballard C, Chaudhuri KR, et al. Parkinson disease-associated cognitive impairment. Nat Rev Dis Prim. 2021;7:47.
- Garcia-Garcia D, Clavero P, Gasca Salas C, Lamet I, Arbizu J, Gonzalez-Redondo R, et al. Posterior parietooccipital hypometabolism may differentiate mild cognitive impairment from dementia in Parkinson's disease. Eur J Nucl Med Mol Imaging. 2012;39:1767–77.
- González-Redondo R, García-García D, Clavero P, Gasca-Salas C, García-Eulate R, Zubieta JL, et al. Grey matter hypometabolism and atrophy in Parkinson's disease with cognitive impairment: a two-step process. Brain. 2014;137:2356–67.
- Rodriguez-Oroz MC, Gago B, Clavero P, Delgado-Alvarado M, Garcia-Garcia D, Jimenez-Urbieta H. The relationship between atrophy and hypometabolism: is it regionally dependent in dementias? Curr Neurol Neurosci Rep. 2015;15:44.
- Nestor PJ. The Lewy body, the hallucination, the atrophy and the physiology. Oxford University Press; 2007.
- Borghammer P. Perfusion and metabolism imaging studies in Parkinson's disease. Dan Med J. 2012;59:B4466.
- Bohnen NI, Yarnall AJ, Weil RS, Moro E, Moehle MS, Borghammer P, et al. Cholinergic system changes in Parkinson's disease: emerging therapeutic approaches. Lancet Neurol. 2022;21:381–92.
- Ballinger EC, Ananth M, Talmage DA, Role LW. Basal forebrain cholinergic circuits and signaling in cognition and cognitive decline. Neuron. 2016;91:1199–218.
- Ovsepian SV, O'Leary VB, Zaborszky L. Cholinergic mechanisms in the cerebral cortex: beyond synaptic transmission. Neuroscientist. 2015;22:238–51.
- Browne SE, Lin L, Mattsson A, Georgievska B, Isacson O. Selective antibodyinduced cholinergic cell and synapse loss produce sustained hippocampal and cortical hypometabolism with correlated cognitive deficits. Exp Neurol. 2001;170:36–47.
- Gelfo F, Petrosini L, Alessandro PG, Bartolo D, Burello L, Vitale E, et al. Cortical metabolic deficits in a rat model of cholinergic basal forebrain degeneration. Neurochem Res. 2013;38:2114–23.
- Grothe MJ, Labrador-Espinosa MA, Jesús S, Macías-García D, Adarmes-Gómez A, Carrillo F, et al. In vivo cholinergic basal forebrain degeneration and cognition in Parkinson's disease: Imaging results from the COPPADIS study. Parkinsonism Relat Disord. 2021;88:68–75.
- Barrett MJ, Sperling SA, Blair JC, Freeman CS, Flanigan JL, Smolkin ME, et al. Lower volume, more impairment: reduced cholinergic basal forebrain grey matter density is associated with impaired cognition in Parkinson disease. J Neurol Neurosurg Psychiatry. 2019;90:1251–6.

Molecular Psychiatry SPRINGER NATURE

- Ray NJ, Bradburn S, Murgatroyd C, Toseeb U, Mir P, Kountouriotis GK, et al. In vivo cholinergic basal forebrain atrophy predicts cognitive decline in de novo Parkinson's disease. Brain. 2018;141:165–76.
- Schulz J, Pagano G, Bonfante JAF, Wilson H, Politis M. Nucleus basalis of Meynert degeneration precedes and predicts cognitive impairment in Parkinson's disease. Brain. 2018:141:1501–16.
- Pereira JB, Hall S, Jalakas M, Grothe MJ, Strandberg O, Stomrud E, et al. Longitudinal degeneration of the basal forebrain predicts subsequent dementia in Parkinson's disease. Neurobiol Dis. 2020;139:104831.
- Labrador-Espinosa MA, Silva-Rodríguez J, Reina-Castillo MI, Mir P, Grothe MJ. Basal forebrain atrophy, cortical thinning, and amyloid-β status in Parkinson's disease-related cognitive decline. Moy Disord. 2023;38:1871–80.
- Postuma RB, Berg D, Stern M, Poewe W, Olanow CW, Oertel W, et al. MDS clinical diagnostic criteria for Parkinson's disease. Mov Disord. 2015;30:1591–601.
- Okkels N, Horsager J, Labrador-Espinosa M, Kjeldsen PL, Damholdt MF, Mortensen J, et al. Severe cholinergic terminal loss in newly diagnosed dementia with Lewy bodies. Brain. 2023;146:3690–704.
- Skorvanek M, Goldman JG, Jahanshahi M, Marras C, Rektorova I, Schmand B, et al. Global scales for cognitive screening in Parkinson's disease: critique and recommendations. Mov Disord. 2018:33:208–18.
- Pagonabarraga J, Kulisevsky J, Llebaria G, García-Sánchez C, Pascual-Sedano B, Gironell A. Parkinson's disease-cognitive rating scale: a new cognitive scale specific for Parkinson's disease. Mov Disord. 2008;23:998–1005.
- Hall S, Janelidze S, Londos E, Leuzy A, Stomrud E, Dage JL, et al. Plasma phosphotau identifies Alzheimer's co-pathology in patients with lewy body disease. Mov Disord. 2021;36:767–71.
- Ashton NJ, Brum WS, Di Molfetta G, Benedet AL, Arslan B, Jonaitis E, et al. Diagnostic accuracy of a plasma phosphorylated tau 217 immunoassay for Alzheimer disease pathology. JAMA Neurol. 2024;81:255–63.
- Periñán MT, Macías-García D, Labrador-Espinosa M, Jesús S, Buiza-Rueda D, Adarmes-Gómez AD, et al. Association of PICALM with cognitive impairment in Parkinson's disease. Mov Disord. 2021;36:118–23.
- Mizutani R, Saiga R, Takekoshi S, Inomoto C, Nakamura N, Itokawa M, et al. A method for estimating spatial resolution of real image in the Fourier domain. J Microsc. 2015;261:57–66.
- 26. Felix C, Alex Z, Barry B. A data-driven approach for estimating the spatial resolution of brain PET images (4301). Neurology. 2020;94:4301.
- Ashburner J. A fast diffeomorphic image registration algorithm. NeuroImage. 2007;38:95–113.
- Fritz H-CJ, Ray N, Dyrba M, Sorg C, Teipel S, Grothe MJ. The corticotopic organization of the human basal forebrain as revealed by regionally selective functional connectivity profiles. Hum Brain Mapp. 2019;40:868–78.
- Grothe MJ, Heinsen H, Amaro E, Grinberg LT, Teipel SJ. Cognitive correlates of basal forebrain atrophy and associated cortical hypometabolism in mild cognitive impairment. Cerebral Cortex. 2016;26:2411–26.
- Silva-Rodríguez J, Labrador-Espinosa MA, Moscoso A, Schöll M, Mir P, Grothe MJ. Characteristics of amnestic patients with hypometabolism patterns suggestive of Lewy body pathology. Brain. 2023;146:4520–31.
- Gonzalez-Escamilla G, Lange C, Teipel S, Buchert R, Grothe MJ. PETPVE12: an SPM toolbox for partial volume effects correction in brain PET – application to amyloid imaging with AV45-PET. NeuroImage. 2017;147:669–77.
- Okkels N, Horsager J, Labrador-Espinosa MA, Hansen FO, Andersen KB, Just K, et al. Distribution of cholinergic nerve terminals in the aged human brain measured with [18 F]FEOBV PET and its correlation with histological data. Neuro-Image. 2023;269:119908.
- Groemping U. Relative importance for linear regression in R: the package relaimpo. J Stat Softw. 2006;17:1–27.
- Imai K, Keele L, Yamamoto T. Identification, inference and sensitivity analysis for causal mediation effects. Stat Sci. 2010;25:51–71.
- Schaefer A, Kong R, Gordon EM, Laumann TO, Zuo X-N, Holmes AJ, et al. Localglobal parcellation of the human cerebral cortex from intrinsic functional connectivity MRI. Cerebral Cortex. 2018:28:3095–114.
- Bohnen NI, Koeppe RA, Minoshima S, Giordani B, Albin RL, Frey KA, et al. Cerebral glucose metabolic features of Parkinson disease and incident dementia: longitudinal study. J Nucl Med. 2011;52:848–55.
- Mesulam MM. The cholinergic innervation of the human cerebral cortex. Prog Brain Res. 2004:145:67–78.
- Jellinger K. Quantitative changes in some subcortical nuclei in aging, Alzheimer's disease and Parkinson's disease. Neurobiol Aging, 1987;8:556–61.
- Liu AKL, Chang RC-C, Pearce RKB, Gentleman SM. Nucleus basalis of Meynert revisited: anatomy, history and differential involvement in Alzheimer's and Parkinson's disease. Acta Neuropathol. 2015;129:527–40.
- Schumacher J, Kanel P, Dyrba M, Storch A, Teipel S, Grothe MJ. Structural and molecular cholinergic imaging markers of cognitive decline in Parkinson's disease. Brain. 2023;146:4964–73.

- 41. Ray NJ, Kanel P, Bohnen NI. Atrophy of the cholinergic basal forebrain can detect presynaptic cholinergic loss in Parkinson's disease. Ann Neurol. 2023;93:991–8.
- 42. Crowley SJ, Kanel P, Roytman S, Bohnen NI, Hampstead BM. Basal forebrain integrity, cholinergic innervation and cognition in idiopathic Parkinson's disease. Brain. 2024;147:1799–1808.
- Khundakar AA, Hanson PS, Erskine D, Lax NZ, Roscamp J, Karyka E, et al. Analysis
 of primary visual cortex in dementia with Lewy bodies indicates GABAergic
 involvement associated with recurrent complex visual hallucinations. Acta Neuropathol Commun. 2016;4:66.
- Patterson L, Firbank MJ, Colloby SJ, Attems J, Thomas AJ, Morris CM. Neuropathological changes in dementia with lewy bodies and the Cingulate Island sign. J Neuropathol Exp Neurol. 2019;78:717–24.
- Higuchi M, Tashiro M, Arai H, Okamura N, Hara S, Higuchi S, et al. Glucose hypometabolism and neuropathological correlates in brains of dementia with Lewy bodies. Exp Neurol. 2000;162:247–56.
- Andersen KB, Hansen AK, Schacht AC, Horsager J, Gottrup H, Klit H, et al. Synaptic density and glucose consumption in patients with Lewy Body Diseases: an [(11) C]UCB-J and [(18) F]FDG PET study. Mov Disord. 2023;38:796–805.
- Albrecht F, Ballarini T, Neumann J, Schroeter ML. FDG-PET hypometabolism is more sensitive than MRI atrophy in Parkinson's disease: a whole-brain multimodal imaging meta-analysis. NeuroImage Clin. 2019;21:101594.
- Lanskey JH, McColgan P, Schrag AE, Acosta-Cabronero J, Rees G, Morris HR, et al. Can neuroimaging predict dementia in Parkinson's disease? Brain. 2018;141:2545–60.
- Svenningsson P, Westman E, Ballard C, Aarsland D. Cognitive impairment in patients with Parkinson's disease: diagnosis, biomarkers, and treatment. Lancet Neurol. 2012;11:697–707.
- Bohnen NI, Muller MLTM, Kotagal V, Koeppe RA, Kilbourn MA, Albin RL, et al. Olfactory dysfunction, central cholinergic integrity and cognitive impairment in Parkinson's disease. Brain. 2010;133:1747–54.
- Van Der Zee S, Müller MLTM, Kanel P, Van Laar T, Bohnen NI. Cholinergic denervation patterns across cognitive domains in Parkinson's disease. Mov Disord. 2021;36:642–50.
- Mori T, Ikeda M, Fukuhara R, Nestor PJ, Tanabe H. Correlation of visual hallucinations with occipital rCBF changes by donepezil in DLB. Neurology. 2006;66:935–7.
- 53. Suantio AM, Huang HL, Kwok CSN, Teo DCH, Nguyen MH. FDG-PET in suspected dementia with Lewy bodies: a case report. BMC Geriatr. 2019;19:150.
- Satoh M, Ishikawa H, Meguro K, Kasuya M, Ishii H, Yamaguchi S. Improved visual hallucination by donepezil and occipital glucose metabolism in dementia with lewy bodies: the Osaki-Tajiri project. Eur Neurol. 2010;64:337–44.
- Baik K, Kim SM, Jung JH, Lee YH, Chung SJ, Yoo HS, et al. Donepezil for mild cognitive impairment in Parkinson's disease. Sci Rep. 2021;11:4734.
- Bohnen NI, Müller MLTM, Kotagal V, Koeppe RA, Kilbourn MR, Gilman S, et al. Heterogeneity of cholinergic denervation in Parkinson's disease without dementia. J Cereb Blood Flow Metab. 2012;32:1609–17.
- Hirano S, Shinotoh H, Shimada H, Ota T, Sato K, Tanaka N, et al. Voxel-based acetylcholinesterase PET study in early and late onset Alzheimer's disease. J Alzheimers Dis. 2018;62:1539–48.
- Richter N, Nellessen N, Dronse J, Dillen K, Jacobs HIL, Langen KJ, et al. Spatial distributions of cholinergic impairment and neuronal hypometabolism differ in MCI due to AD. NeuroImage Clin. 2019;24:101978.
- Grothe MJ, Teipel SJ. Spatial patterns of atrophy, hypometabolism, and amyloid deposition in Alzheimer's disease correspond to dissociable functional brain networks. Hum Brain Mapp. 2016;37:35–53.
- Mielke MM, Dage JL, Frank RD, Algeciras-Schimnich A, Knopman DS, Lowe VJ, et al. Performance of plasma phosphorylated tau 181 and 217 in the community. Nat Med. 2022;28:1398–405.
- 61. Gharbi-Meliani A, Dugravot A, Sabia S, Regy M, Fayosse A, Schnitzler A, et al. The association of APOE ε4 with cognitive function over the adult life course and incidence of dementia: 20 years follow-up of the Whitehall II study. Alzheimers Res Ther. 2021;13:5.
- Jansen WJ, Janssen O, Tijms BM, Vos SJB, Ossenkoppele R, Visser PJ, et al. Prevalence estimates of amyloid abnormality across the Alzheimer disease clinical spectrum. JAMA Neurol. 2022;79:228–43.
- Coughlin DG, Hurtig HI, Irwin DJ. Pathological Influences on clinical heterogeneity in Lewy body diseases. Mov Disord. 2020;35:5–19.
- Peter J, Mayer I, Kammer T, Minkova L, Lahr J, Klöppel S, et al. The relationship between cholinergic system brain structure and function in healthy adults and patients with mild cognitive impairment. Sci Rep. 2021;11:1–7.
- Frey KA, Bohnen NILJ. Molecular imaging of neurodegenerative Parkinsonism. PET Clin. 2021;16:261–72.
- Apostolova I, Lange C, Frings L, Klutmann S, Meyer PT, Buchert R. Nigrostriatal degeneration in the cognitive part of the striatum in Parkinson disease is associated with frontomedial hypometabolism. Clin Nuclear Med. 2020;45:95–99.
- Orso B, Arnaldi D, Girtler N, Brugnolo A, Doglione E, Mattioli P, et al. Dopaminergic and serotonergic degeneration and cortical [18F]fluorodeoxyglucose positron emission tomography in De Novo Parkinson's disease. Mov Disord. 2021;36:2293–302.

SPRINGER NATURE Molecular Psychiatry

ACKNOWLEDGEMENTS

The authors would like to thank the participants in this study for their contribution to science and the Instituto de Biomedicina de Sevilla and the Hospital Universitario Virgen del Rocío for the research resources provided.

AUTHOR CONTRIBUTIONS

MJG and PM contributed to the study conceptualization and design. NO, LMD, JH, AMCG, ElC, MSE, DMG, SJ, AAG, EOL, FC, FRL, DGS, and PB contributed to the data collection and material preparation. MALE, JSR, NO, SCL, PFR, and JFMR were involved in pre-processing and preparing the data for the analysis. The analyses were performed by MALE and JSR. The first draft of the manuscript was written by MALE and JSR. All authors commented on previous versions of the manuscript. All authors read and approved the final manuscript.

FUNDING

This work was supported by the Spanish Ministry of Science and Innovation (RTC2019-007150-1, PID2021-127034OA-I00), the Instituto de Salud Carlos III-Fondo Europeo de Desarrollo Regional (ISCIII-FEDER) (PI16/01575, PI18/01898, PI19/01576, Pl20/00613, Pl21/01875, Pl22/01704), the Consejería de Economía, Innovación, Ciencia y Empleo de la Junta de Andalucía (CVI-02526, CTS-7685), the Consejería de Salud y Bienestar Social de la Junta de Andalucía (PI-0471-2013, PE-0210-2018, PI-0459-2018, PE-0186-2019), the Consejería de Transformación Económica, Industria, Conocimiento y Universidades de la Junta de Andalucía (PY20_00896, P20_00903), and the Fundación Alicia Koplowitz. Several authors of this publication are members of the European Reference Network for Rare Neurological Diseases (project ID 739510). M.A.L.E. is supported by a PhD scholarship (VI-PPIT-US) from the University of Seville (USE-19094-G). J.S.R. is supported by the "Sara Borrell" program (CD21/ 00067) of the ISCIII-FEDER. M.J.G. is supported by the "Miguel Servet" program (CP19/ 00031) of the ISCIII-FEDER. N.O. is supported by the Danish Parkinson's Disease Association and the Health Research Foundation of Central Denmark Region. L.M.D. is supported by the "Río Hortega" program (CM21/00051) of the ISCIII-FEDER. D.M.G. is supported by the "Juan Rodés" program (JR22/00073) of the ISCIII-FEDER.

COMPETING INTERESTS

The authors declare no competing interests.

ETHICS APPROVAL

This study was performed in line with the principles of the Declaration of Helsinki. Approval was granted by the Ethics Committee of the University Hospital 'Virgen del Rocío' (approval number: 2158-N-20).

CONSENT FOR PUBLICATION

Informed consent was obtained from all individual participants included in the study.

ADDITIONAL INFORMATION

Supplementary information The online version contains supplementary material available at https://doi.org/10.1038/s41380-024-02842-9

Correspondence and requests for materials should be addressed to Pablo Mir or Michel I. Grothe

Reprints and permission information is available at http://www.nature.com/reprints

Publisher's note Springer Nature remains neutral with regard to jurisdictional claims in published maps and institutional affiliations.

Springer Nature or its licensor (e.g. a society or other partner) holds exclusive rights to this article under a publishing agreement with the author(s) or other rightsholder(s); author self-archiving of the accepted manuscript version of this article is solely governed by the terms of such publishing agreement and applicable law.

Molecular Psychiatry SPRINGER NATURE